A Thumbwheel Mechanism for APOA1 Activation of LCAT Activity in HDL

Allison L. Cooke, Jamie Morris, John T. Melchior, Scott E. Street, W. Gray Jerome, Rong Huang, Andrew B. Herr, Loren E. Smith, Jere P. Segrest, Alan T. Remaley, Amy S. Shah, Thomas B. Thompson, and W. Sean Davidson

Online Supplement

SUPPLEMENTARY METHODS

Electron Microscopy

Particles were negatively stained with 2% phosphotungstic acid at pH 5.6 and imaged with a ThermoFisher (formerly FEI) Technai T-12 electron microscope (Vanderbilt University). For quantification of particle diameters, >100 particles from 3 separate preparations of each type of particle were selected using an unbiased sampling grid.

Chemical cross-linking of rHDL

Particles generated with WT or mutant APOA1 were cross-linked with BS^3-H12/D12 (Creative Molecules Inc., spacer arm length= 11.4 Å) at a cross-linker to protein ratio of 50:1 (mol/mol). The cross-linking reaction was performed at 4°C for 16 h and the reaction was quenched by addition of Tris-HCl to a final concentration of 35 mM. The particles were dialyzed 3x4L against 50 mM ammonium bicarbonate (pH 8.1), for downstream preparation for MS.

MS analysis of rHDL

Dried peptides (100 µg) were reconstituted in 15 µl of 0.1% formic acid in water and 5 µl of sample was applied to an ACQUITY UPLC C18 reverse phase column (Waters) maintained at 60°C using an Infinity 1290 autosampler and HPLC (Agilent). Peptides were eluted at 0.1 ml/min using a mobile phase gradient from 95% phase A (FA/H2O 0.1/99.9, v/v) to 32% phase B (FA/ACN 0.1/99.9 v/v) for 120 min followed by 32% B to 50% B for 2 min. Column cleaning was performed by varying the mobile phase gradient to 90% B for 10 min and the column was re-equilibrated at 95% A for 10 min. Peptides were introduced to the MS using a Jet Stream source (Agilent) as previously described (1). Spectra were acquired using an iFunnel Q-TOF (Agilent) operating in positive ion mode. Precursors were limited to acquisition of ions with a charge state ≥ 3+ and required a minimum of 1500 counts. Each cycle acquired the 20 most intense precursors which were fragmented with a variable collision energy (CE) dependent on the precursor mass-to-charge (m/z) ratio: CE = k* (m/z) +b, with a slope (k) of 4 and an offset (b) of -2 for 3+ ions and -4 for ions > 3+. MS/MS spectra were acquired until 45,000 total counts were collected or a maximum accumulation time of 0.33 s. Mascot generic files (MGF) were generated using MassHunter Qualitative Analysis Software (v. B.07.00, Agilent). MS/MS peaks were limited to the top 150 peaks by height and precursors were limited to a maximum assigned charge state of 6+.

Analysis of rHDL/LCAT interaction by NDGGE rHDL

rHDL and LCAT were cross-linked with Bis (sulfo-succinimidyl)suberate (BS^3, Pierce, spacer arm length= 11.4 Å) at a 4:1 (mol/mol) ratio of APOA1: LCAT, and 100:1 (mol/mol) ratio of BS^3: APOA1. Cross-linking was performed for 2 h at 4°C, and the reaction was quenched with 30mM Tris-HCl. NDGGE (4-15%) stained with Coomassie Blue was used to analyze rHDL/LCAT complex formation. Bands were analyzed by densitometry using ImageJ software (v. 1.47t). Bands were then excised from the gel and prepared for nanoLC-MS/MS analysis (see *MS analysis of the rHDL:LCAT complex in Methods)*. Each section was analyzed by nano LC-MS/MS and searched against all entries in the SwissProt_20161222 database via Mascot (v. 2.2.07).

SUPPLEMENTARY TABLE 1

Reaction velocity (nmol CE/hr) of LCAT activation by rHDL particles.

Oxidizing Conditions (S-S)

rHDL	**LCAT activity (nmol CE/hr)**	**% of Wild-type (WT)**
WT	0.19 ± 0.02	100
K133C (5/5)	0.26 ± 0.02	135
K206C (5/2)	0.06 ± 0.00	30
K195C (5/1)	0.05 ± 0.00	25

Reducing Conditions (-SH HS-)

rHDL	**LCAT activity (nmol CE/hr)**	**% of Wild-type (WT)**
WT	0.31 ± 0.01	100
K133C (5/5)	0.36 ± 0.00	114
K206C (5/2)	0.26 ± 0.03	82
K195C (5/1)	0.25 ± 0.02	79

SUPPLEMENTARY TABLE 2

Mutations in APOA1 that decrease LCAT activation and have normal ABCA1 mediated cholesterol efflux.

Helix	Mutation	LCAT activation	ABCA1 mediated cholesterol efflux
4	ΔK107 (Helsinki)	*Rall et al. 1984 (4), Tilly-Kiesi et al.1995 (5)*	*Gonzalez et al. 2008 (6)*
	E110K	*Hoang et al. 2003 (7)*	*Takada et al.1990 (8)*
	E110A/E111A	*Chroni et al. 2004 (9), Chroni et al. 2005 (10)*	*Chroni et al. 2005*
	D102A/D103A	*Chroni et al. 2005*	*Chroni et al. 2004*
6	P143A	*Sviridov et al. 2000 (11)*	*Sviridov et al. 2002 (12)*
	R149V	*Sviridov et al. 2000*	*Sviridov et al. 2002*
	R149A	*Koukos et al. 2007 (13)*	*Koukos et al. 2007*
	R151C (Paris)	*Daum et al. 1999 (14), Koukos et al. 2007*	*Koukos et al. 2007*
	V156E (Oita)	*Huang et al. 1998 (15), Cho et al. 2001 (16), Hoang et al. 2003*	*Sviridov et al. 2002*
	L159R (Fin)	*Miettinen et al. 1997 (17), Cigliano et al. 2008 (18)*	*Miettinien et al.1997*
	R160L	*Daum et al. 1999 (19), Cho et al. 2001, Koukos et al. 2007*	*Koukos et al. 2007*
	R160V/H162A	*Chroni et al. 2005*	*Chroni et al. 2004*
	H162Q	*Moriyama et al.1996 (20), Hoang et al. 2003*	*Sviridov et al. 2002*
7	P165R	*von Eckardstein et al. 1989 (21), Daum et al. 1999*	*Daum et al. 1999*
	P165A	*Gu et al. 2016(22)*	*Gu et al. 2016*
	Y166F	*Shao et al. 2008(23), Wu et al. 2007(24), Gu et al. 2016*	*Gu et al. 2016*
	Y166A	*Gu et al. 2016*	*Gu et al. 2016*
	Y166E	*Gu et al. 2016*	*Gu et al. 2016*
	Y166N	*Gu et al. 2016*	*Gu et al. 2016*
	S167A	*Gu et al. 2016*	*Gu et al. 2016*
	D168A	*Gu et al. 2016*	*Gu et al. 2016*
	R173C (Milano)	*Weisgraber et al. 1980 (25), Weisgraber et al. 1983 (26), Calabresi et al.1997 (27)*	*Weibel et al. 2007 (28)*

SUPPLEMENTARY LEGENDS AND FIGURES

Supplementary Figure 1. WT and Cys-mutant rHDL analyzed by electron microscopy. Black bar measures 50 nm. a) WT rHDL, b) K133C rHDL, c) K206C rHDL, d) K195C rHDL.

Supplementary Figure 2. Representative total compound chromatograms and MS1 spectra of cross-links identified in rHDL particles. Total compound chromatogram (TCC, large graph) and MS1 spectra (small graph) showing the instrument counts based on elution time and mass-charge ratio, respectively, for the identification of cross-link (XL) a) K77-K195 (5/5), b) K59-K208 (5/5), c) K96-K118 (5/2), and d) K106-K118 (5/2) in WT, K133C, K206C, and K195C rHDL particles.

Supplementary Figure 3. Substrate-velocity curve of LCAT activation by WT rHDL. WT rHDL particles were generated with [^{3}H]- free cholesterol as indicated in "Methods". WT rHDL (0-1.4 µM) was incubated with a constant concentration of LCAT (0.02 µM) for 30 min. at 37°C. Results were plotted based on cholesteryl ester generated per hour as a function of WT rHDL mass.

Supplementary Figure 4. LCAT binding WT APOA1 and Cys-mutant rHDL assessed by chemical cross-linking. A 4:1 ratio of rHDL and LCAT was incubated with BS^3, a lysine-to-lysine cross-linker, at a 100:1 molar ratio of cross-linker to APOA1 for 16 h at 4°C. NDGGE stained with Coomassie blue was used to analyze cross-link formation. XL indicates samples with (+) or without (-) added BS^3 cross-linker. As a control, WT XL + LCAT XL indicates WT rHDL cross-linked with BS^3 before being cross-linked again to LCAT. A band identified in all cross-linked samples was excised from the gel, reduced with DTT, alkylated with iodoacetamide and digested with trypsin as indicated in Methods. Each section was analyzed by nano LC-MS/MS and searched against all entries in the SwissProt_20161222 database via Mascot (v. 2.2.07).

Supplementary Figure 5. Flow scheme of rHDL and LCAT binding analysis with SPR. a) CM5 sensorchips were used for binding analysis. A mouse anti-APOA1 monoclonal antibody (4H1, residues 2-8) was immobilized on the sensorchip. rHDL particles were coupled to 4H1 and 0.2- 55 µM LCAT was injected over rHDL. b) Flow schemes of sensorchip 1 and 2. Flow cell (FLC) 1 of both chips were used as reference surfaces by coupling a mouse anti-ubiquitin (anti-UB) monoclonal antibody to the surface. rHDL particles coupled to 4H1 on FLCs 2-4 of the sensorchip

1 were WT, K206C, and K195C, respectively. Sensorchip 2 was coupled with a 7.8 nm WT APOA1 particle as a negative control. FLC 3 and 4 contained K133C and WT rHDL particles respectively. WT rHDL on sensorchip 2 was coupled to a different FC than sensorchip 1 in order to account for any differences in rHDL position on FCs. Four buffer blanks were included randomly throughout LCAT injections. LCAT injections were performed in duplicate: the first from increasing to decreasing concentrations, and the second from decreasing to increasing concentrations.

Supplementary Figure 6. Localization of APOA1 point mutations that adversely affect LCAT activity without impairing ABCA1 mediated cholesterol efflux. Depiction of two APOA1 molecules arranged in a 2D anti-parallel stacked ring (gray and white). APOA1 molecules are shown divided into 10 helices (H1-H10), with the N-terminus depicted as an octagon, and the C-terminus as a black curved line. Residue numbers (1-243) of APOA1 are shown at the cusp between helices. Natural and bioengineered mutations are indicated in line callouts and are referenced in **Supp.Table 2**. Green and blue shaded areas represent two independent locations on an HDL disc that may activate LCAT. Adapted from Sorci-Thomas et al. (2) and Zannis et al.(3).

SUPPLEMENTARY FIGURE 1

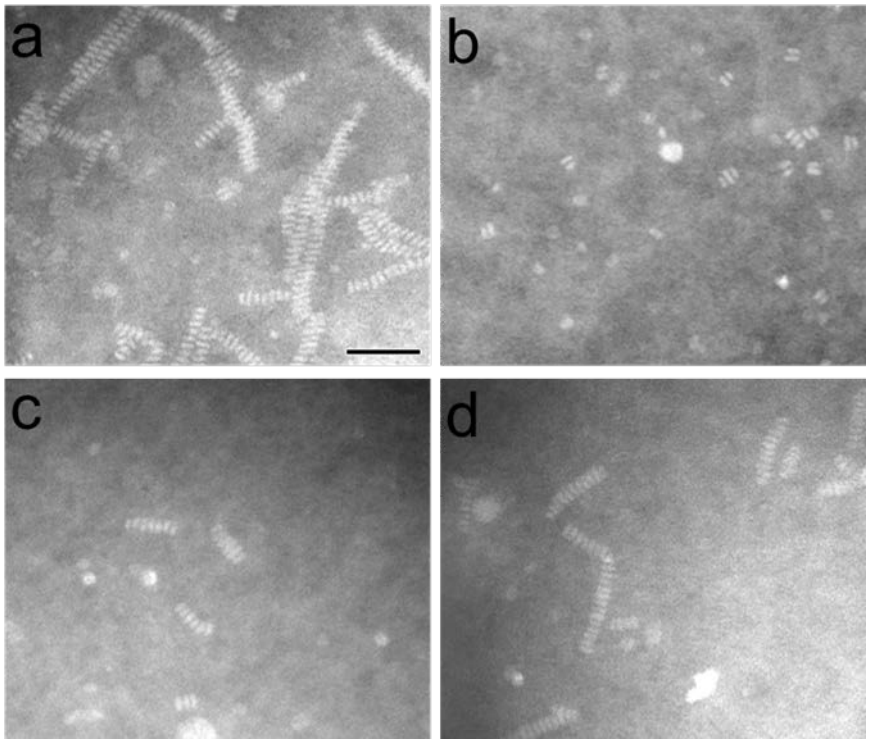

SUPPLEMENTARY FIGURE 2

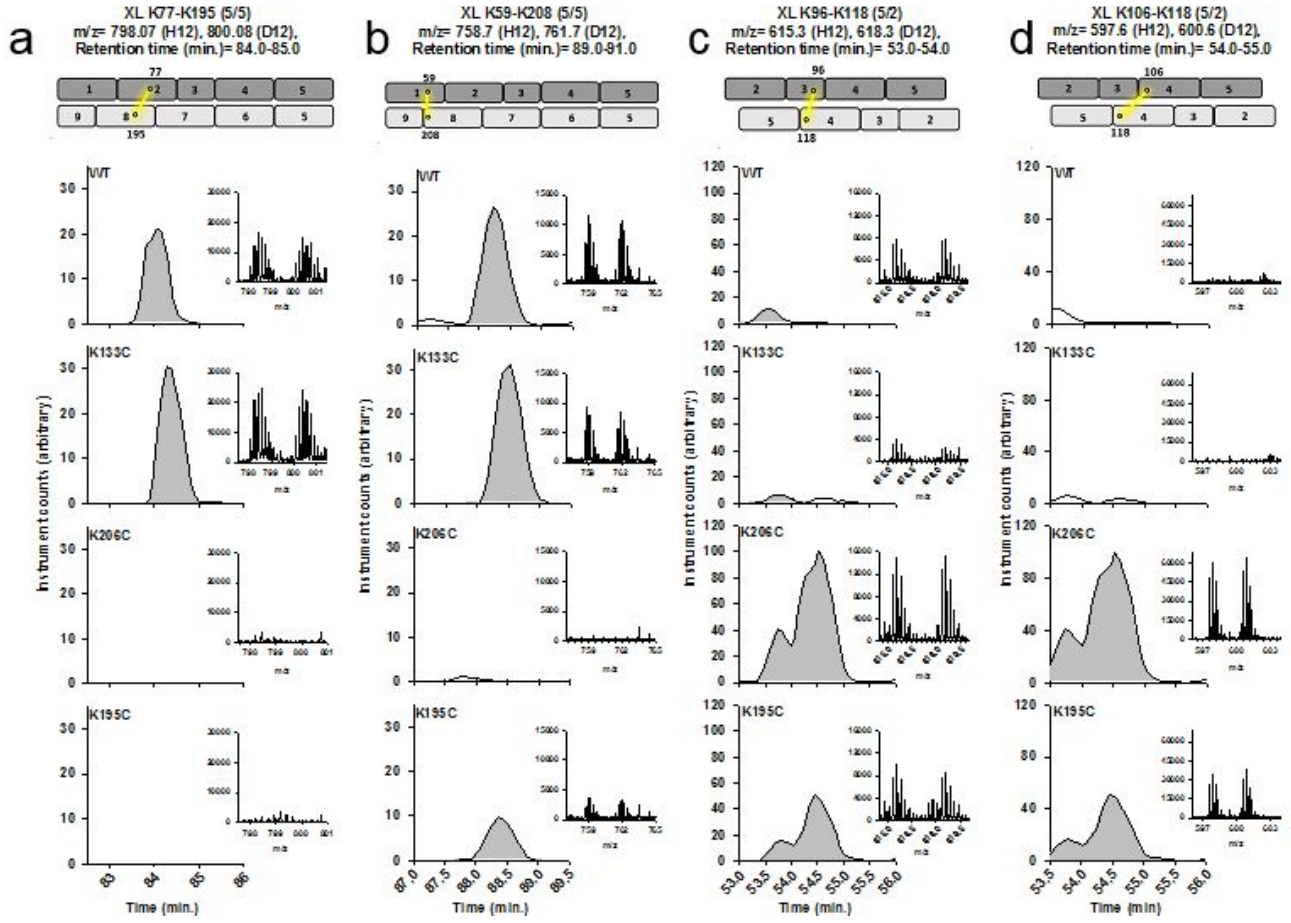

SUPPLEMENTARY FIGURE 3

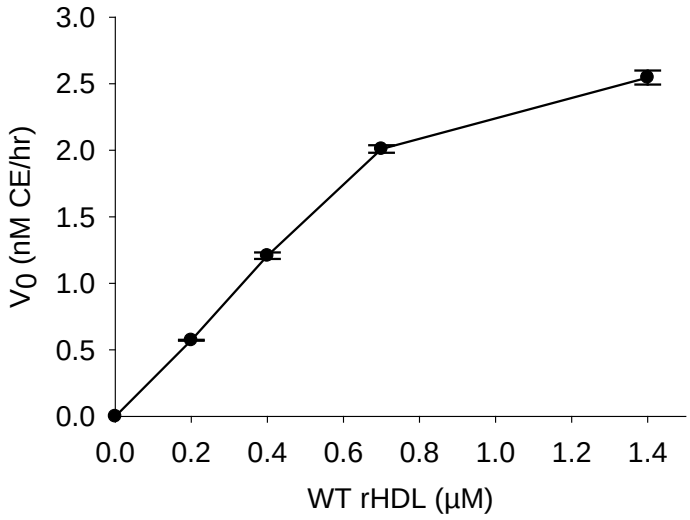

SUPPLEMENTARY FIGURE 4

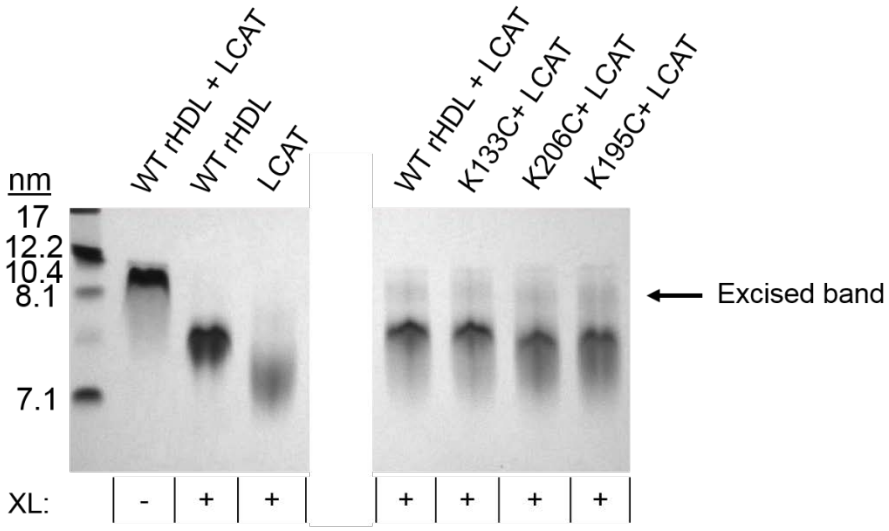

SUPPLEMENTARY FIGURE 5

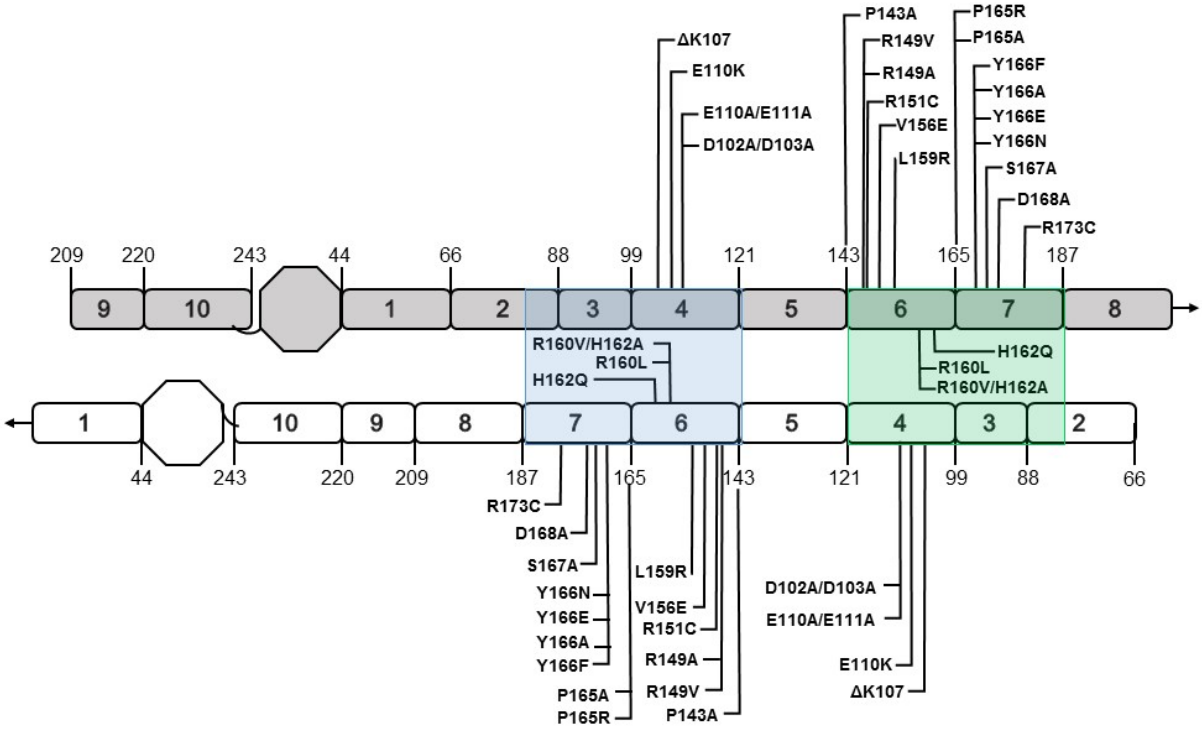

SUPPLEMENTARY FIGURE 6

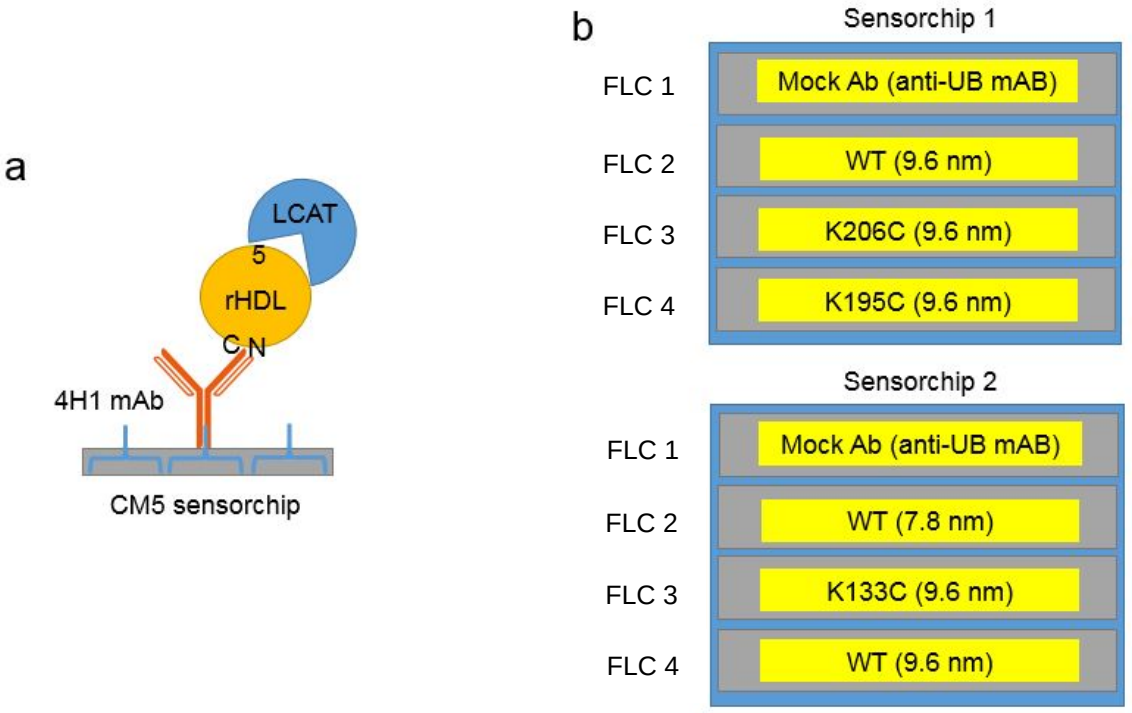

SUPPLEMENTARY REFERENCES

(1) Gonzalez Fernandez-Nino, S. M., A. M. Smith-Moritz, L. J. Chan, P. D. Adams, J. L. Heazlewood, and C. J. Petzold. 2015. Standard flow liquid chromatography for shotgun proteomics in bioenergy research.*Front. Bioeng. Biotechnol.* **3:** 44.

(2) Sorci-Thomas, M. G., M. J. Thomas. 2002. The effects of altered apolipoprotein A-I structure on plasma HDL concentration. *Trends Cardiovasc. Med.* **12:** 121-128.

(3) Zannis, V. I., A. Chroni, and M. Krieger. 2006. Role of apoA-I, ABCA1, LCAT, and SR-BI in the biogenesis of HDL. *J. Mol. Med. (Berl)* **84:** 276-294.

(4) Rall, S. C., K. H. Weisgraber, R. W. Mahley, Y. Ogawa, C. J. Fielding, G. Utermann, J. Haas, A. Steinmetz, H. J. Menzel, and G. Assmann. 1984. Abnormal lecithin:cholesterol acyltransferase activation by a human apolipoprotein A-I variant in which a single lysine residue is deleted. *J. Biol. Chem.* **259:** 10063-10070.

(5) Tilly-Kiesi, M., Q. Zhang, S. Ehnholm, J. Kahri, S. Lahdenpera, C. Ehnholm, and M. R. Taskinen. 1995. ApoA-IHelsinki (Lys107-->0) associated with reduced HDL cholesterol and LpA-I:A-II deficiency. *Arterioscler. Thromb. Vasc. Biol.* **15:**1294-1306.

(6) Gonzalez, M. C., J. D. Toledo, M. A. Tricerri, and H. A. Garda. 2008. The central type Y amphipathic alpha-helices of apolipoprotein AI are involved in the mobilization of intracellular cholesterol depots. *Arch. Biochem. Biophys.* **473:** 34-41.

(7) Hoang, A., W. Huang, J. Sasaki, and D. Sviridov. 2003. Natural mutations of apolipoprotein A-I impairing activation of lecithin:cholesterol acyltransferase. *Biochim. Biophys. Acta* **1631:** 72-76.

(8) Takada, Y., J. Sasaki, S. Ogata, T. Nakanishi, Y. Ikehara, and K. Arakawa. 1990. Isolation and characterization of human apolipoprotein A-I Fukuoka (110 Glu----Lys). A novel apolipoprotein variant. *Biochim. Biophys. Acta* **1043:** 169-176.

(9) Chroni, A., H. Y. Kan, K. E. Kypreos, I. N. Gorshkova, A. Shkodrani, and V. I. Zannis. 2004. Substitutions of glutamate 110 and 111 in the middle helix 4 of human apolipoprotein A-I (apoA-I) by alanine affect the structure and in vitro functions of apoA-I and induce severe hypertriglyceridemia in apoA-I-deficient mice. *Biochemistry* **43:** 10442-10457.

(10) Chroni, A., A. Duka, H. Y. Kan, T. Liu, and V. I. Zannis. 2005. Point mutations in apolipoprotein A-I mimic the phenotype observed in patients with classical lecithin:cholesterol acyltransferase deficiency. *Biochemistry* **44:** 14353-14366.

(11) Sviridov, D., A. Hoang, W. H. Sawyer, and N. H. Fidge. 2000. Identification of a sequence of apolipoprotein A-I associated with the activation of Lecithin:Cholesterol acyltransferase. *J. Biol. Chem.* **275:** 19707-19712.

(12) Sviridov, D., A. Hoang, W. Huang, and J. Sasaki. 2002. Structure-function studies of apoA-I variants: site-directed mutagenesis and natural mutations. *J. Lipid Res.* **43:** 1283-1292.

(13) Koukos, G., A. Chroni, A. Duka, D. Kardassis, and V. I. Zannis. 2007. LCAT can rescue the abnormal phenotype produced by the natural ApoA-I mutations (Leu141Arg)Pisa and (Leu159Arg)FIN. *Biochemistry* **46:** 10713-10721.

(14) Daum, U., C. Langer, N. Duverger, F. Emmanuel, P. Benoit, P. Denefle, A. Chirazi, P. Cullen, P. H. Pritchard, E. Bruckert, G. Assmann, and A. von Eckardstein. 1999. Apolipoprotein A-I (R151C)Paris is defective in activation of lecithin: cholesterol acyltransferase but not in initial lipid binding, formation of reconstituted lipoproteins, or promotion of cholesterol efflux. *J. Mol. Med. (Berl)* **77:** 614-622.

(15) Huang, W., J. Sasaki, A. Matsunaga, H. Nanimatsu, K. Moriyama, H. Han, M. Kugi, T. Koga, K. Yamaguchi, and K. Arakawa. 1998. A novel homozygous missense mutation in the apo A-I gene with apo A-I deficiency. *Arterioscler. Thromb. Vasc. Biol.* **18:** 389-396.

(16) Cho, K. H., D. M. Durbin, and A. Jonas. 2001. Role of individual amino acids of apolipoprotein A-I in the activation of lecithin:cholesterol acyltransferase and in HDL rearrangements. *J. Lipid Res.* **42:** 379-389.

(17) Miettinen, H. E., M. Jauhiainen, H. Gylling, S. Ehnholm, A. Palomaki, T. A. Miettinen, and K. Kontula. 1997. Apolipoprotein A-IFIN (Leu159-->Arg) mutation affects lecithin cholesterol acyltransferase activation and subclass distribution of HDL but not cholesterol efflux from fibroblasts. *Arterioscler. Thromb. Vasc. Biol.* **17:** 3021-3032.

(18) Cigliano, L., L. D. D'Andrea, B. Maresca, M. Serino, A. Carlucci, A. Salvatore, M. S. Spagnuolo, G. Scigliuolo, C. Pedone, and P. Abrescia. 2008. Relevance of the amino acid conversions L144R (Zaragoza) and L159P (Zavalla) in the apolipoprotein A-I binding site for haptoglobin. *Biol. Chem.* **389:** 1421-1426.

(19) Daum, U., T. P. Leren, C. Langer, A. Chirazi, P. Cullen, P. H. Pritchard, G. Assmann, and A. von Eckardstein. 1999. Multiple dysfunctions of two apolipoprotein A-I variants, apoA-I(R160L)Oslo and apoA-I(P165R), that are associated with hypoalphalipoproteinemia in heterozygous carriers. *J. Lipid Res.* **40:** 486-494.

(20) Moriyama, K., J. Sasaki, A. Matsunaga, Y. Takada, M. Kagimoto, and K. Arakawa. 1996. Identification of two apolipoprotein variants, A-I Karatsu (Tyr 100-->His) and A-I Kurume (His 162-->Gln). *Clin. Genet.* **49:** 79-84.

(21) von Eckardstein, A., H. Funke, A. Henke, K. Altland, A. Benninghoven, and G. Assmann. 1989. Apolipoprotein A-I variants. Naturally occurring substitutions of proline residues affect plasma concentration of apolipoprotein A-I. *J. Clin. Invest.* **84:** 1722-1730.

(22) Gu, X., Z. Wu, Y. Huang, M. A. Wagner, C. Baleanu-Gogonea, R. A. Mehl, J. A. Buffa, A. J. DiDonato, L. B. Hazen, P. L. Fox, V. Gogonea, J. S. Parks, J. A. DiDonato, and S. L. Hazen. 2016. A Systematic Investigation of Structure/Function Requirements for the Apolipoprotein A-I/Lecithin Cholesterol Acyltransferase Interaction Loop of High-density Lipoprotein. *J. Biol. Chem.* **291:** 6386-6395.

(23) Shao, B., G. Cavigiolio, N. Brot, M. N. Oda, and J. W. Heinecke. 2008. Methionine oxidation impairs reverse cholesterol transport by apolipoprotein A-I. *Proc. Natl. Acad. Sci. U. S. A.* **105:** 12224-12229.

(24) Wu, Z., M. A. Wagner, L. Zheng, J. S. Parks, J. M. Shy 3rd, J. D. Smith, V. Gogonea, and S. L. Hazen. 2007. The refined structure of nascent HDL reveals a key functional domain for particle maturation and dysfunction. *Nat. Struct. Mol. Biol.* **14:** 861-868.

(25) Weisgraber, K. H., T. P. Bersot, R. W. Mahley, G. Franceschini, and C. R. Sirtori. 1980. A-Imilano apoprotein. Isolation and characterization of a cysteine-containing variant of the A-I apoprotein from human high density lipoproteins. *J. Clin. Invest.* **66:** 901-907.

(26) Weisgraber, K. H., S. C. Rall, T. P. Bersot, R. W. Mahley, G. Franceschini, and C. R. Sirtori. 1983. Apolipoprotein A-IMilano. Detection of normal A-I in affected subjects and evidence for a cysteine for arginine substitution in the variant A-I. *J. Biol. Chem.* **258:** 2508-2513.

(27) Calabresi, L., G. Franceschini, A. Burkybile, and A. Jonas. 1997. Activation of lecithin cholesterol acyltransferase by a disulfide-linked apolipoprotein A-I dimer. *Biochem. Biophys. Res. Commun.* **232:** 345-349.

(28) Weibel, G. L., E. T. Alexander, M. R. Joshi, D. J. Rader, S. Lund-Katz, M. C. Phillips, and G. H. Rothblat. 2007. Wild-type ApoA-I and the Milano variant have similar abilities to stimulate cellular lipid mobilization and efflux. *Arterioscler. Thromb. Vasc. Biol.* **27:** 2022-2029.